

# The GLP-1 analogue lixisenatide decreases atherosclerosis in insulin-resistant mice by modulating macrophage phenotype

Ángela Vinué<sup>1</sup> · Jorge Navarro<sup>1,2,3</sup> · Andrea Herrero-Cervera<sup>1</sup> · Marta García-Cubas<sup>1</sup> · Irene Andrés-Blasco<sup>1</sup> · Sergio Martínez-Hervás<sup>1,4,5</sup> · José T. Real<sup>1,4,5</sup> · Juan F. Ascaso<sup>1,4,5</sup> · Herminia González-Navarro<sup>1,5</sup>

Received: 25 January 2017 / Accepted: 10 May 2017 / Published online: 12 June 2017  
© Springer-Verlag Berlin Heidelberg 2017

## Abstract

**Aims/hypothesis** Recent clinical studies indicate that glucagon-like peptide-1 (GLP-1) analogues prevent acute cardiovascular events in type 2 diabetes mellitus but their mechanisms remain unknown. In the present study, the impact of GLP-1 analogues and their potential underlying molecular mechanisms in insulin resistance and atherosclerosis are investigated.

**Methods** Atherosclerosis development was evaluated in *ApoE*<sup>-/-</sup>*Irs2*<sup>+/-</sup> mice, a mouse model of insulin resistance, the metabolic syndrome and atherosclerosis, treated with the GLP-1 analogues lixisenatide or liraglutide. In addition, studies in *ApoE*<sup>-/-</sup>*Irs2*<sup>+/-</sup> mice and mouse-derived macrophages treated with lixisenatide were performed to investigate the potential inflammatory intracellular pathways.

**Results** Treatment of *ApoE*<sup>-/-</sup>*Irs2*<sup>+/-</sup> mice with either lixisenatide or liraglutide improved glucose metabolism and

blood pressure but this was independent of body weight loss. Both drugs significantly decreased atheroma plaque size. Compared with vehicle-treated control mice, lixisenatide treatment generated more stable atheromas, with fewer inflammatory infiltrates, reduced necrotic cores and thicker fibrous caps. Lixisenatide-treated mice also displayed diminished IL-6 levels, proinflammatory Ly6C<sup>high</sup> monocytes and activated T cells. In vitro analysis showed that, in macrophages from *ApoE*<sup>-/-</sup>*Irs2*<sup>+/-</sup> mice, lixisenatide reduced the secretion of the proinflammatory cytokine IL-6 accompanied by enhanced activation of signal transducer and activator of transcription (STAT) 3, which is a determinant for M2 macrophage differentiation. STAT1 activation, which is essential for M1 phenotype, was also diminished. Furthermore, atheromas from lixisenatide-treated mice showed higher arginase I content and decreased expression of inducible nitric oxide synthase, indicating the prevalence of the M2 phenotype within plaques.

**Conclusions/interpretation** Lixisenatide decreases atheroma plaque size and instability in *ApoE*<sup>-/-</sup>*Irs2*<sup>+/-</sup> mice by reprogramming macrophages towards an M2 phenotype, which leads to reduced inflammation. This study identifies a critical role for this drug in macrophage polarisation inside plaques and provides experimental evidence supporting a novel mechanism of action for GLP-1 analogues in the reduction of cardiovascular risk associated with insulin resistance.

Ángela Vinué and Jorge Navarro contributed equally to this work.

**Electronic supplementary material** The online version of this article (doi:10.1007/s00125-017-4330-3) contains peer-reviewed but unedited supplementary material, which is available to authorised users.

✉ Herminia González-Navarro  
herminia.gonzalez@uv.es

<sup>1</sup> Institute of Health Research-INCLIVA, Avda Menéndez Pelayo 4, 46010 Valencia, Spain

<sup>2</sup> Clinic Hospital and Department of Medicine, University of Valencia, Institute of Health Research-INCLIVA, Valencia, Spain

<sup>3</sup> CIBER Epidemiología y Salud Pública (CIBERESP), Madrid, Spain

<sup>4</sup> Endocrinology and Nutrition Department, Clinic Hospital and Department of Medicine, University of Valencia, Valencia, Spain

<sup>5</sup> Centro de Investigación Biomédica en Red de Diabetes y Enfermedades Metabólicas Asociadas (CIBERDEM), Madrid, Spain

**Keywords** Atherosclerosis · GLP-1 · Inflammation · Macrophage · STAT

## Abbreviations

ApoB Apolipoprotein B  
ApoE Apolipoprotein E  
CVD Cardiovascular disease

GLP-1	Glucagon-like peptide-1
iNOS	Inducible nitric oxide synthase
IR	Insulin resistance
LPS	Lipopolysaccharide
MAPK	Mitogen activated protein kinase
MCP1	Monocyte chemoattractant protein 1
STAT	Signal transducer and activator of transcription
VSMC	Vascular smooth muscle cell

## Introduction

Type 2 diabetes mellitus and the metabolic syndrome are major risk factors for developing cardiovascular disease (CVD) [1]; individuals with vulnerable atheroma plaques are at highest risk. These plaques are prone to rupture, promoting life-threatening acute cardiovascular events, and are characterised by the presence of an inflammatory infiltrate comprised of macrophages and T cells [2]. Studies in mouse models of insulin resistance (IR) and atherosclerosis have shown that IR in vascular-wall cells promotes atheroma plaque instability via several mechanisms [1, 3–5]. IR increases macrophage apoptosis and reduces vascular smooth muscle cell (VSMC) survival, favouring the thinning of plaque fibrous caps and increasing the size of their necrotic cores [1, 6]. Changes in plaque stability in IR have also been attributed to the activity and effects of inflammatory mediators [6, 7], which recruit monocytes and T lymphocytes and favour the formation of inflammatory necrotic cores. Therefore, therapeutic strategies designed to reduce atheroma inflammation and to stabilise plaques are a high priority in the prevention of acute events [8].

Analogues derived from the glucagon-like peptide-1 (GLP-1) hormone are effective in the treatment of type 2 diabetes and obesity [9]. Moreover, preclinical testing has demonstrated that these analogues have cardioprotective effects in rat models of myocardial injury [10, 11] and protect against atherosclerosis in the apolipoprotein E (apoE)-deficient mouse model [12]. The recent ELIXA (Evaluation of Lixisenatide in Acute Coronary Syndrome) and LEADER (Liraglutide Effect and Action in Diabetes: Evaluation of Cardiovascular Outcome Results) clinical trials [13, 14] indicate that treatments with GLP-1 analogues are safe [14] and represent useful therapies for the prevention of death caused by cardiovascular events [13] in type 2 diabetes. However, the mechanisms by which GLP1 analogues might provide protection against CVD remain largely unknown. Thus, more work is required to expand our understanding of the effects of incretin-based therapies in the different cardiovascular system pathways and to gain mechanistic insights for use in advanced personalised therapies.

In this study, we explored the impact of the GLP-1 analogues lixisenatide and liraglutide on cardiometabolic

dysbalance and atherosclerosis using a mouse model featuring IR, the metabolic syndrome and atherosclerosis. This strain, *ApoE<sup>-/-</sup>Irs2<sup>+/-</sup>*, combines apoE deficiency with a partial IRS2 deficiency. In addition, plaque vulnerability and the inflammation associated with this vulnerability were examined and the potential molecular mechanisms underlying lixisenatide treatment were explored.

## Methods

**Mice and diets** Animal care was in accordance with our institutional guidelines and followed the 2010/63/EU directive from the European Parliament. *ApoE<sup>-/-</sup>* (C57BL/6J; Charles River, L'Arbresle, France) and *Irs2<sup>+/-</sup>* (C57BL/6J) mice were crossed to generate *ApoE<sup>-/-</sup>Irs2<sup>+/-</sup>* mice, which were identified by genotyping [4]. Mice were fed a regular chow diet (2014C Tekland Global 14% wt/wt protein; Harlan Iberica, Barcelona, Spain) and at 2 months they were placed on an atherogenic diet for 2 months (10.8% wt/wt total fat, 0.75% wt/wt cholesterol; S4892-E010; Sniff, Soest, Germany). Mice were randomised and blindly assigned to receive lixisenatide ( $n = 15$ ; Lyxumia; Sanofi, Paris, France) at 10  $\mu\text{g}/\text{kg}$  body weight per day, liraglutide (Victoza; Novo Nordisk, Bagsvaerd, Denmark) ( $n = 10$ ) at 400  $\mu\text{g}/\text{kg}$  body weight per day or vehicle ( $n = 13$ ) through a subcutaneously implanted osmotic minipump (ALZET 2004; Charles River) during the last month of the diet. Doses for lixisenatide and liraglutide were chosen based on the previously reported optimal doses obtained from pharmacokinetic and drug-clearance studies in rodents described for lixisenatide [11, 15, 16] and liraglutide [12, 17–19]. Blood pressure was measured in conscious mice using a non-invasive tail-cuff system (LE5002 Pressure Meter; Panlab, Barcelona, Spain) as previously described [20].

**Metabolic measurements in mice** Plasma lipid levels in overnight-fasted mice were measured using enzymatic procedures (Wako, Zaragoza, Spain). HDL-cholesterol was determined after precipitation of apolipoprotein B (apoB) with dextran sulfate [21]. GTT and ITT analysis were performed as described [22, 23]. For detailed description of the tests, see the electronic supplementary material [ESM] [Methods](#).

**Quantification of atherosclerosis burden** Mice were killed by cervical dislocation and whole aorta and hearts were harvested for analysis. Atherosclerosis was determined in whole-mounted aorta fixed with 4% vol./vol. paraformaldehyde–PBS and stained with Oil Red-O (0.2% wt/vol. in 80% vol./vol. methanol) by en face morphometric analysis (Image J, <https://imagej.nih.gov/ij/>) and in H&E-stained aortic cross-sections of paraffin-embedded heart as the lesion area (in

mm<sup>2</sup>) in the aortic root and as the intima–media ratio in the ascending aorta [24].

**Immunohistopathological analysis of atheromas** Masson's trichrome staining was used to determine the collagen content, necrotic core area and fibrous cap thickness of atheromas as described [6]. The content of arginase I, inducible nitric oxide synthase (iNOS), macrophages, VSMCs and T lymphocytes in atheromas was determined by immunostainings as described [6]. Macrophage proliferation rate and apoptosis and macrophages expressing arginase I and iNOS were analysed by double immunofluorescence. A detailed description of the immunostainings can be found in ESM [Methods](#).

**ELISA** Plasma was isolated by centrifugation of heparinised blood (10 U heparin/ml) and TNF $\alpha$ , monocyte chemoattractant protein-1 (MCP1) and IL-6 were measured using the DuoSet ELISA kits (R&D Systems, Minneapolis, MN, USA).

**Flow cytometry measurements** Leucocyte analysis was performed in 10  $\mu$ l of heparinised whole blood as reported [25]. For detailed description of the flow cytometry analysis, see ESM [Methods](#).

**Inflammatory properties of bone-marrow macrophages** Murine bone-marrow-derived macrophages were obtained from the femoral bone marrow of mice killed by cervical dislocation. Cells were differentiated for 7 days with 10% vol./vol. FBS–DMEM (Lonza, Basel, Switzerland) supplemented with 10% vol./vol. L929-cell conditioned medium (LCM; a source of macrophage colony-stimulating factor) [24] in the presence of 40 nmol/l of lixisenatide or saline (154 mmol/l NaCl). For the last 24 h, or 6 h before analysis, the macrophages were challenged with lipopolysaccharide (LPS; 100 ng/ml) or vehicle. Cytokine secretion in the supernatant fraction was evaluated by ELISA and protein expression by western blot analysis. Three independent experiments were performed in triplicate.

**Western blot analysis** Protein extracts were obtained by homogenising cellular pellets of macrophages as previously described [6, 23]. For a detailed description, see ESM [Methods](#).

**Statistical analysis** Quantitative variables are shown as the mean  $\pm$  SEM. Differences among two groups were evaluated using Student's *t* test. All data obtained during the experiments were analysed unless these data were out of range of the standard curve or samples were lost during the experimental procedure. Multiple comparisons were performed using one-way ANOVA followed by Bonferroni's or Tukey's post hoc analysis and two-way ANOVA followed by a Bonferroni's post hoc

test (GraphPad Software, La Jolla, CA, USA). Differences were considered statistically significant if  $p \leq 0.05$ .

## Results

**Metabolic characterisation of vehicle-, liraglutide- and lixisenatide-treated *Apoe*<sup>-/-</sup>*Irs2*<sup>+/-</sup> mice fed an atherogenic diet** The body weights of vehicle-, liraglutide- and lixisenatide-treated *Apoe*<sup>-/-</sup>*Irs2*<sup>+/-</sup> mice were significantly increased after the atherogenic diet (Fig. 1a); no difference was found between treatments. Systolic and diastolic blood pressure were significantly decreased in lixisenatide-treated *Apoe*<sup>-/-</sup>*Irs2*<sup>+/-</sup> mice compared with liraglutide- and vehicle-treated mice (Fig. 1b, c). Compared with vehicle treatment, liraglutide treatment decreased systolic blood pressure (Fig. 1b). Fasting basal glucose was similar among groups (Fig. 1d) but, compared with vehicle-treated mice, liraglutide- and lixisenatide-treated *Apoe*<sup>-/-</sup>*Irs2*<sup>+/-</sup> mice had significantly decreased fasting insulin levels (Fig. 1e).

Further carbohydrate metabolism characterisation using the GTT (Fig. 2a) revealed improved glucose tolerance, measured as the AUC<sub>glucose</sub>, in lixisenatide-treated *Apoe*<sup>-/-</sup>*Irs2*<sup>+/-</sup> mice compared with vehicle-treated controls. The glucose-stimulated insulin release during the GTT (Fig. 2b), expressed as AUC<sub>insulin</sub>, showed decreased insulin secretion in liraglutide- and lixisenatide-treated mice compared with vehicle-treated controls. The ITT also demonstrated higher insulin sensitivity in liraglutide- and lixisenatide-treated mice, as revealed by a decrease in the AUC<sub>glucose</sub> (Fig. 2c). Interestingly, lipid analysis showed that neither liraglutide nor lixisenatide treatment had an effect on total cholesterol, apoB-cholesterol, HDL-cholesterol or triacylglycerol levels in *Apoe*<sup>-/-</sup>*Irs2*<sup>+/-</sup> mice (Fig. 2d–g). Therefore, as expected, liraglutide and lixisenatide improve carbohydrate metabolism and blood pressure in these mice without affecting lipid metabolism.

**Lixisenatide treatment in atherogenic-diet-fed *Apoe*<sup>-/-</sup>*Irs2*<sup>+/-</sup> mice diminishes the atherosclerosis burden and produces more stable plaques** Analysis of whole-mounted aortas (Fig. 3a) demonstrated that, compared with vehicle-treated *Apoe*<sup>-/-</sup>*Irs2*<sup>+/-</sup> mice, liraglutide- and lixisenatide-treated mice exhibited smaller atheromas in the aortic arch region (Fig. 3b) without significant changes in the thoracic aorta (Fig. 3c). Similarly, the lesion size in cross-sections of hearts was also reduced in the aortic root (Fig. 3d), ascending aorta (Fig. 3e) and the aorta (Fig. 3f) of lixisenatide-treated *Apoe*<sup>-/-</sup>*Irs2*<sup>+/-</sup> mice compared with vehicle-treated mice. Atheroma analysis in cross-sections from liraglutide-treated mice showed a more modest reduction in size, which did not reach statistical significance (Fig. 3d–f). Given that our mouse model had a better

**Fig. 1** Characterisation of vehicle-, liraglutide- and lixisenatide-treated *ApoE<sup>-/-</sup>Irs2<sup>+/-</sup>* mice. **(a)** The body weight (BW) of mice before and after the diet. **(b, c)** Systolic **(b)** and diastolic **(c)** blood pressure of mice. **(d, e)** Fasting plasma glucose **(d)** and insulin levels **(e)** in mice. Statistical analysis was performed using two-way ANOVA **(a)** and one-way ANOVA test **(b–e)** followed by Bonferroni's post hoc test. White bars, vehicle-treated mice; grey bars, liraglutide-treated mice; black bars, lixisenatide-treated mice. \* $p < 0.05$ , \*\*\* $p < 0.001$  as indicated

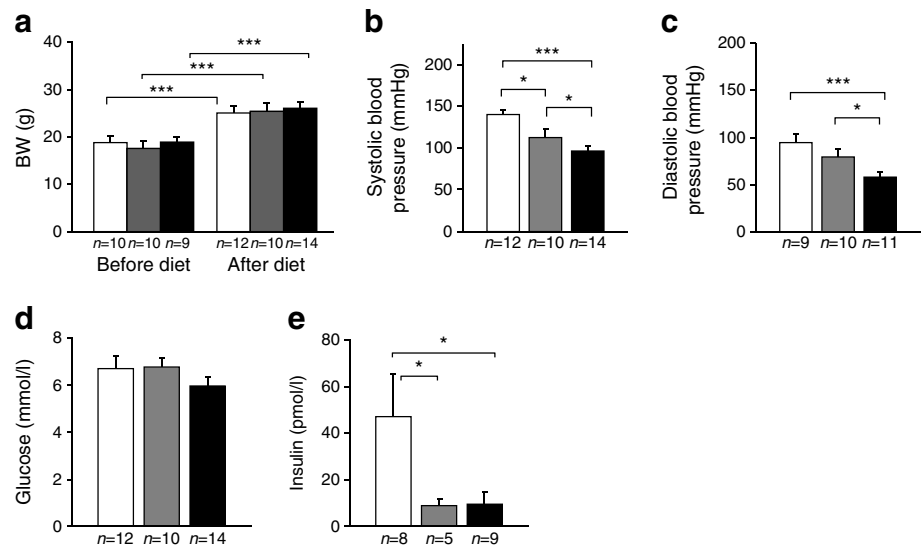


**Fig. 2** Metabolic analysis of vehicle-, liraglutide- and lixisenatide-treated *ApoE<sup>-/-</sup>Irs2<sup>+/-</sup>* mice. **(a)** Plasma glucose levels during the GTT and  $AUC_{\text{glucose}}$  generated from the glucose curve during the test. **(b)** Plasma glucose-stimulated insulin levels during the GTT and the  $AUC_{\text{insulin}}$  generated from the insulin measurements during the test. **(c)** Plasma glucose levels during the ITT and  $AUC_{\text{glucose}}$  generated from the glucose curve during the test in 4 h fasted mice. **(d–g)** Total cholesterol (T-chol, **d**), ApoB-cholesterol (ApoB-chol, **e**), HDL-cholesterol (HDL-chol, **f**) and triacylglycerol (**g**) plasma levels in the three groups of mice. Statistical analysis was performed using one-way ANOVA test followed by Bonferroni's post hoc test. White bars and circles, vehicle-treated mice; grey bars and black triangles, liraglutide-treated mice; black bars and circles, lixisenatide-treated mice. \* $p < 0.05$ , \*\* $p < 0.01$  as indicated

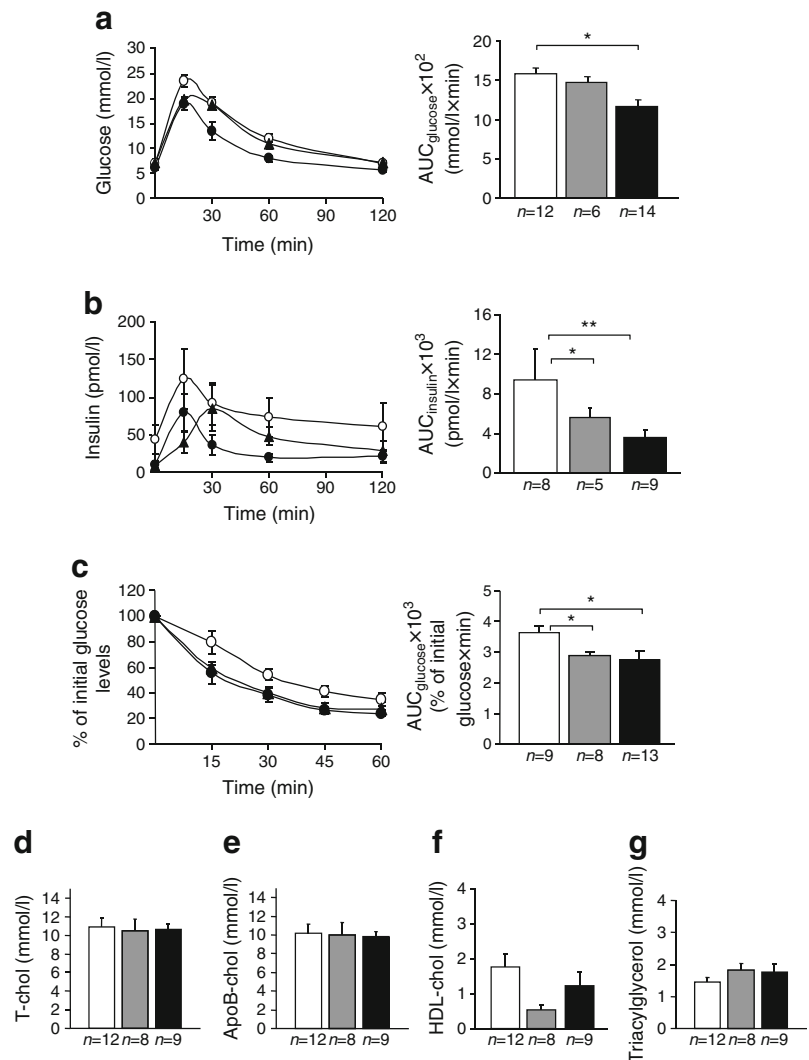
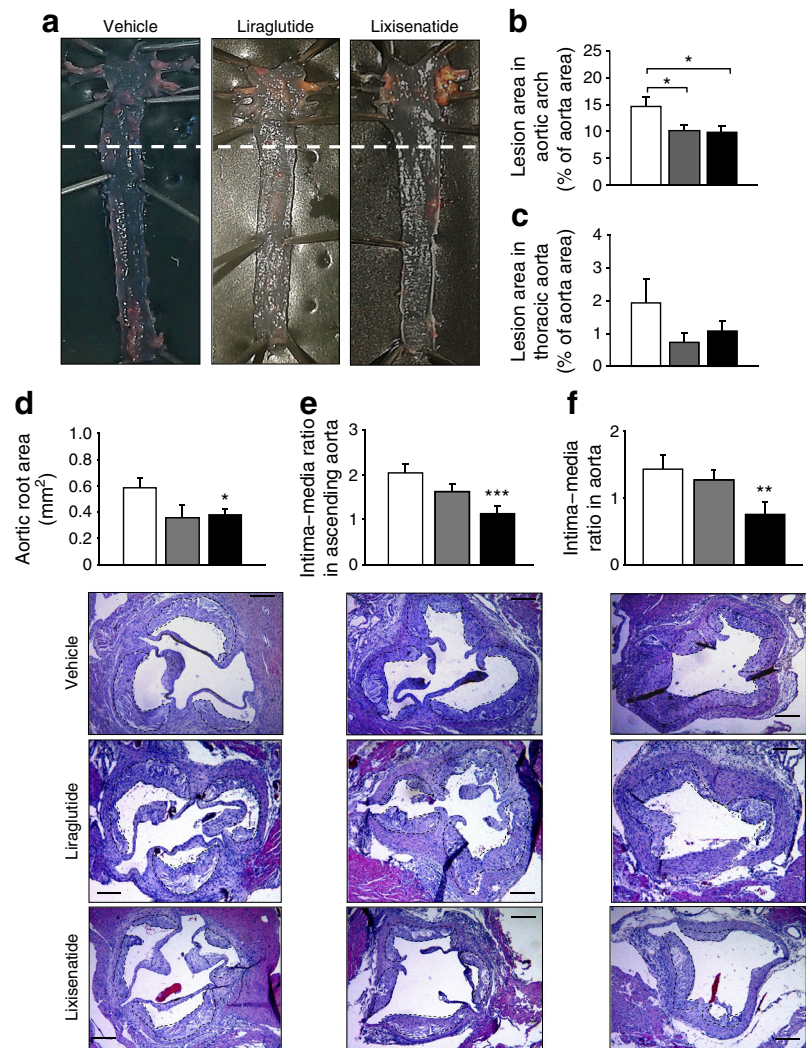


**Fig. 3** Analysis of atherosclerotic lesions in vehicle-treated, liraglutide-treated and lixisenatide-treated *Apoe*<sup>-/-</sup>*Irs2*<sup>+/-</sup> mice. (a–c) Representative photographs of Oil-Red-O-stained whole-mounted aortas (a) were used for quantification of lesion area in the aortic arch (b) and thoracic aorta (c). (d–f) Representative images from H&E-stained cross-sections of hearts were used for quantification of atheroma lesion size measured as area in the aortic root (d) and as the intima–media ratio in the ascending aorta (e) and in aorta (f). The dashed line in (a) limits the aortic arch region (above) and the thoracic aorta region (below). The dashed lines in the images in (d, e, f) delineate the limits of the lesion. Statistical analysis was performed using one-way ANOVA followed by Bonferroni's post hoc test (a–e). White bars, vehicle-treated mice, *n* = 12 or 13; grey bars, liraglutide-treated mice, *n* = 7–9; black bars, lixisenatide-treated mice, *n* = 14 or 15. Scale bar, 200  $\mu$ m. \**p* < 0.05, \*\**p* < 0.01, \*\*\**p* < 0.001 vs vehicle



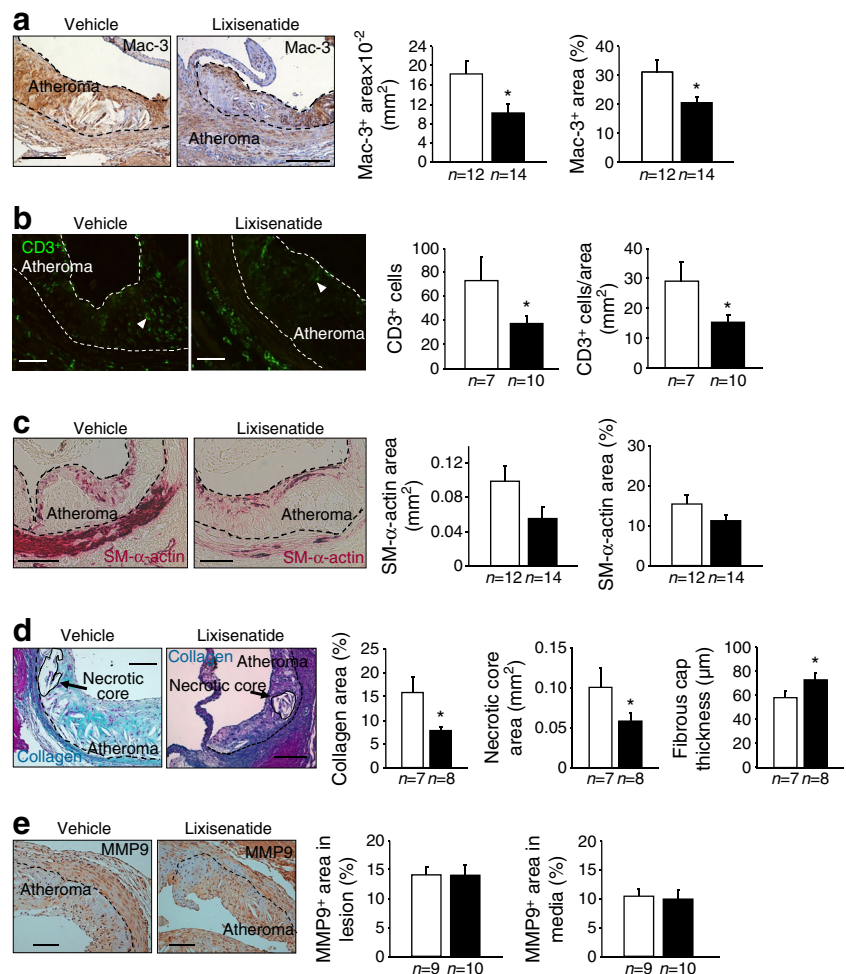
response to lixisenatide treatment, further studies were performed in lixisenatide-treated mice.

Analysis of the composition of atheroma plaques (Fig. 4) revealed a reduced content of macrophages measured as both absolute and relative macrophage area (Fig. 4a). The T lymphocyte content, measured as total number of CD3<sup>+</sup> cells and as number of CD3<sup>+</sup> cells per lesion area (Fig. 4b), was also decreased in atheromas from lixisenatide-treated *Apoe*<sup>-/-</sup>*Irs2*<sup>+/-</sup> mice compared with vehicle-treated mice. No changes were observed in VSMC content between mouse groups (Fig. 4c). Examination of plaque stability characteristics revealed decreased collagen content (Fig. 4d), reduced necrotic core area (Fig. 4d) and increased fibrous cap thickness (Fig. 4d) in lixisenatide-treated mice. No differences were observed in matrix metalloproteinase 9 content in the lesion or in the media (Fig. 4e) when comparing the two groups of mice. Thus, lixisenatide treatment decreases atherosclerosis and inflammatory infiltration and promotes acquisition of some characteristics of plaque stability.

**Effect of lixisenatide treatment on macrophage survival in *Apoe*<sup>-/-</sup>*Irs2*<sup>+/-</sup> mouse atheromas** The decreased macrophage content in lesions might be explained by changes in cellular proliferation and apoptosis—key events in plaque growth and stability. However, analysis of proliferation and apoptosis in vivo did not reveal any differences between lixisenatide- and vehicle-treated *Apoe*<sup>-/-</sup>*Irs2*<sup>+/-</sup> mouse atheromas (Fig. 5a–d).

**Lixisenatide treatment decreases systemic inflammation in atherogenic-diet-fed *Apoe*<sup>-/-</sup>*Irs2*<sup>+/-</sup> mice** Given that lixisenatide treatment markedly decreased inflammatory infiltrates in plaques, we next investigated inflammation. Analysis of circulating leucocytes showed a decreased percentage of lymphocytes and an increase in the percentage of neutrophils in lixisenatide-treated *Apoe*<sup>-/-</sup>*Irs2*<sup>+/-</sup> mice compared with vehicle-treated mice (Fig. 6a). The percentage of monocytes was slightly decreased in lixisenatide-treated *Apoe*<sup>-/-</sup>*Irs2*<sup>+/-</sup> mice but the difference was not significant (Fig. 6a).

**Fig. 4** Effect of lixisenatide on atheroma plaque composition in *Apoe<sup>-/-</sup>Irs2<sup>+/-</sup>* mice. Neointimal content of: macrophages, measured as area and as percentage (a), using Mac-3 as a marker; T lymphocytes, measured as total cell number and as relative cell number, using CD3 as a marker (b); and VSMCs measured as area and as percentage, using SM- $\alpha$ -actin as a marker (c). Arrowheads in b indicate CD3<sup>+</sup> stained cells. (d) Representative Masson trichrome stain of atheroma and quantification of neointimal collagen content (percentage), necrotic core area and fibrous cap thickness. Representative images of atheroma and quantification of matrix metalloproteinase 9 (MMP9)-positive area (percentage) in the lesion and in the media of aortic cross-sections (e). The dashed lines in images delineate the limits of the media and lesions and solid lines delineate the limits of representative necrotic cores. Statistical analysis was performed using Student's *t* test. White bars, vehicle-treated mice; black bars, lixisenatide-treated mice. Scale bars, 100  $\mu$ m (a, c, d, e) or 50  $\mu$ m (b). \**p* < 0.05 vs vehicle



Monocyte subpopulation analysis, however, showed that lixisenatide treatment effectively diminished the proinvasive and proinflammatory Ly6C<sup>hi</sup> subset without changing the other monocyte subpopulations in *Apoe<sup>-/-</sup>Irs2<sup>+/-</sup>* mice (Fig. 6b). Compared with the vehicle-treated mice, the lixisenatide-treated *Apoe<sup>-/-</sup>Irs2<sup>+/-</sup>* mice displayed reduced percentages of CD3<sup>+</sup>CD69<sup>+</sup> (Fig. 6d) and CD8<sup>+</sup>CD69<sup>+</sup> (Fig. 6h) activated T cells without changing the other T cell subsets (Fig. 6c, e, f, g). Analysis of proinflammatory cytokines in circulating plasma revealed decreased IL-6 levels in lixisenatide-treated *Apoe<sup>-/-</sup>Irs2<sup>+/-</sup>* mice (Fig. 6k) without changes in MCP1 or TNF $\alpha$  levels (Fig. 6i, j). Therefore, reduced lesion size and inflammatory infiltrate in lixisenatide-treated mice are associated with decreased circulating inflammatory cells and mediators.

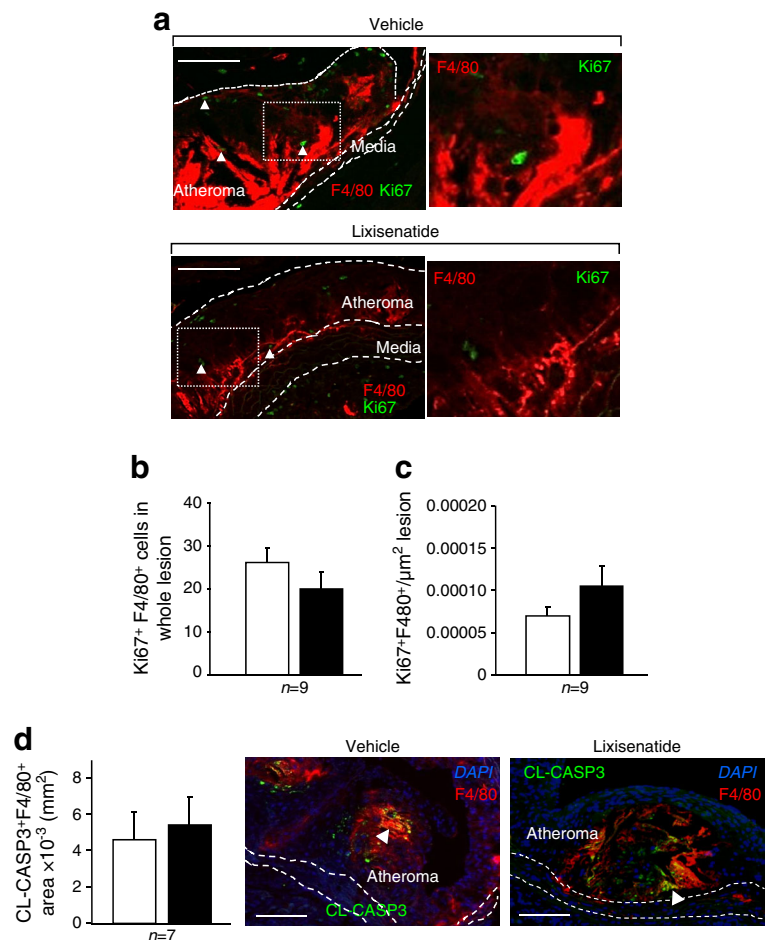
**Lixisenatide decreases the inflammatory properties of *Apoe<sup>-/-</sup>Irs2<sup>+/-</sup>* mouse macrophages** To investigate whether lixisenatide modulated the inflammatory macrophage phenotype, we explored its effect on the differentiation and activation of *Apoe<sup>-/-</sup>Irs2<sup>+/-</sup>* mouse macrophages.

Analysis of cytokine secretion revealed that lixisenatide treatment had no effect on MCP1 (Fig. 7a) or TNF $\alpha$

(Fig. 7b) levels following 6 h stimulation with LPS; however, IL-6 levels in LPS-stimulated macrophages were decreased when compared with vehicle-treated macrophages (Fig. 7c). Compared with basal conditions, 6 h stimulation with LPS augmented the secretion of the all three proinflammatory cytokines, MCP1, TNF $\alpha$  and IL-6 (Fig. 7a–c), in both lixisenatide- and vehicle-treated *Apoe<sup>-/-</sup>Irs2<sup>+/-</sup>* mouse macrophages. After 24 h stimulation with LPS, cytokine secretion was similar between lixisenatide- and vehicle-treated *Apoe<sup>-/-</sup>Irs2<sup>+/-</sup>* mouse macrophages; MCP1, TNF $\alpha$  and IL-6 cytokines were increased in both lixisenatide- and vehicle-treated macrophages compared with unstimulated control counterparts (ESM Fig. 1a–c).

Next, we investigated signal transducer and activator of transcription (STAT) proteins, which are a determinant for macrophage M1/M2 differentiation. Protein expression analysis showed decreased levels of the activated phosphoSTAT1, which is essential for acquisition of M1 phenotype, in 6 h LPS-stimulated lixisenatide-treated macrophages (Fig. 7d) compared with vehicle-treated cells. Analysis of phosphoSTAT3 protein, which is associated with the anti-inflammatory M2 response in macrophages, was significantly

**Fig. 5** Proliferation rate and apoptosis in atheromas from lixisenatide- and vehicle-treated *Apoe*<sup>-/-</sup>*Irs2*<sup>+/-</sup> mice. **(a)** Representative images of atheroma plaques showing double Ki67<sup>+</sup>F4/80<sup>+</sup> staining in vehicle- and lixisenatide-treated cells. Proliferation rate of macrophages within lesions, expressed as the absolute cell number **(b)** and as the number of cells per lesion area **(c)**, measured as double Ki67<sup>+</sup>F4/80<sup>+</sup> cells in atheroma plaques. **(d)** Representative images of atheromas and analysis of apoptosis of macrophages within atheroma plaques, determined as area of double CL-caspase-3<sup>+</sup>F4/80<sup>+</sup>. Arrowheads indicate double Ki67<sup>+</sup>F4/80<sup>+</sup> **(a)** and CL-caspase-3<sup>+</sup>F4/80<sup>+</sup> **(d)** stained areas. The dashed lines delineate the limits of the media. Statistical analysis was performed using Student's *t* test. White bars, vehicle-treated mice; black bars, lixisenatide-treated mice. Scale bars, 100  $\mu$ m. Magnification  $\times 2.5$



augmented in lixisenatide-treated *Apoe*<sup>-/-</sup>*Irs2*<sup>+/-</sup> mouse macrophages in basal conditions and after 6 h stimulation with LPS (Fig. 7d). No differences in phosphoSTAT1 or phosphoSTAT3 levels were observed between lixisenatide- and vehicle-treated macrophages after 24 h LPS stimulation (Fig. 7e). Stimulation with LPS resulted in increased phosphoSTAT1 after 6 h in vehicle-treated macrophages (Fig. 7d) and after 24 h in lixisenatide-treated macrophages (Fig. 7e) compared with basal conditions. PhosphoSTAT3 was augmented after both 6 h (Fig. 7d) and 24 h (Fig. 7e) of LPS stimulation in lixisenatide-treated macrophages compared with unstimulated lixisenatide-treated macrophages. Macrophage phenotype has been reported to be modulated by activation of the stress mitogen activated protein kinase (MAPK) [26, 27]. However, no significant changes were observed in the protein expression of the activated forms of the downstream MAPK phosphoERK, phospho38 or phosphoSAPK/JNK (ESM Fig. 2a–c).

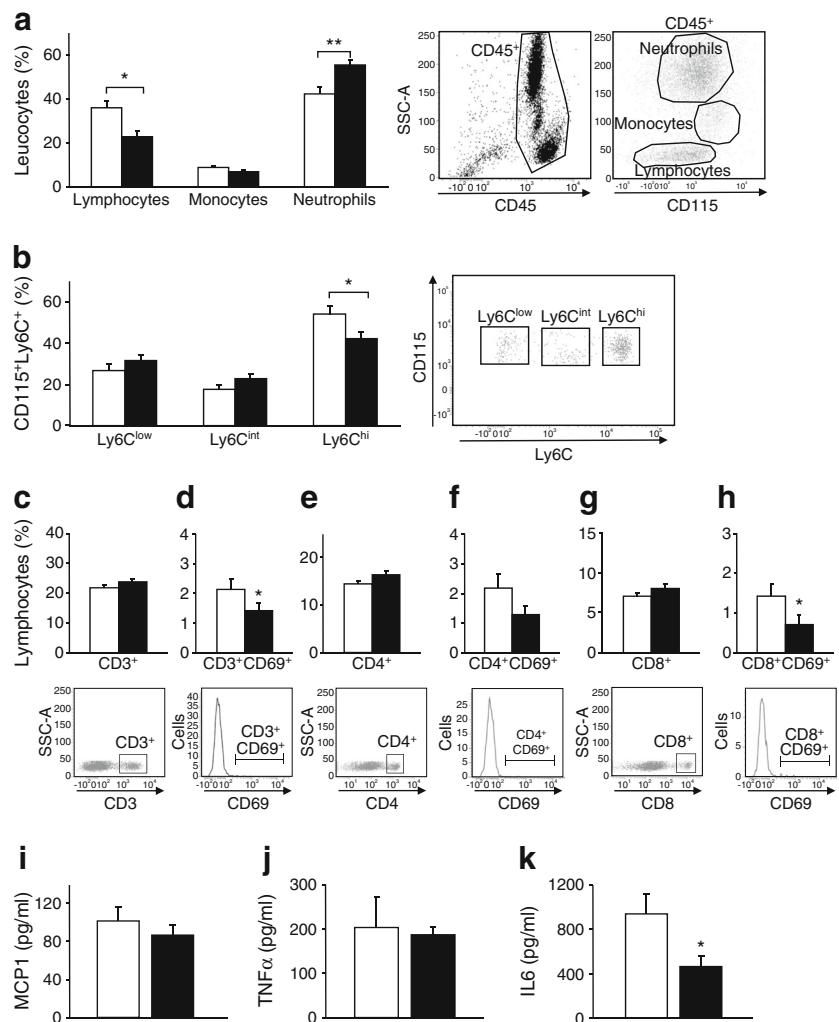
Consistent with these findings, protein expression analysis also demonstrated that lixisenatide treatment decreased the levels of the M1 macrophage marker iNOS in 6 h LPS-stimulated macrophages (Fig. 8a) when compared with vehicle treatment. This difference was not observed after 24 h

stimulation with LPS (Fig. 8b). Compared with basal conditions, increased iNOS protein levels were observed in vehicle-treated macrophages upon 6 h and 24 h stimulation with LPS (Fig. 8a, b) and in lixisenatide-treated macrophages only after 24 h LPS stimulation (Fig. 8b). Lixisenatide-treated macrophages also displayed higher protein levels of the M2 macrophage marker arginase I both in basal conditions and in 24 h LPS-stimulated macrophages (Fig. 8b) compared with vehicle-treated macrophages. No changes were observed in arginase I expression following 6 h of LPS stimulation (Fig. 8a).

These results indicate that lixisenatide affects macrophage reprogramming during differentiation by modulating the STAT signalling pathway, facilitating an anti-inflammatory M2 phenotype with decreased proinflammatory cytokine secretion.

**Lixisenatide treatment modulates macrophage polarisation in vivo in *Apoe*<sup>-/-</sup>*Irs2*<sup>+/-</sup> mouse atheroma plaques** Next, we evaluated the action of lixisenatide on macrophage reprogramming in vivo. The *Apoe*<sup>-/-</sup>*Irs2*<sup>+/-</sup> mice displayed an increase in arginase I in plaques following lixisenatide treatment compared with vehicle treatment (Fig. 8e). In

**Fig. 6** The effect of lixisenatide treatment on systemic inflammation in *Apoe<sup>-/-</sup>Irs2<sup>+/-</sup>* mice. **(a)** Percentages of circulating lymphocytes, monocytes and neutrophils for both treatments. Leucocytes were identified as CD45<sup>+</sup> cells by flow cytometry. **(b)** Circulating monocytes identified as CD115<sup>+</sup> cells and as Ly6C<sup>low</sup>, Ly6C<sup>int</sup>- and Ly6C<sup>hi</sup>-monocyte subsets in mouse blood. Circulating **(c)** total and **(d)** activated T lymphocytes identified as CD3<sup>+</sup> and CD3<sup>+</sup>CD69<sup>+</sup> cells, respectively. Quantification of **(e)** CD4<sup>+</sup> and **(g)** CD8<sup>+</sup> T cells and activated **(f)** CD4<sup>+</sup>CD69<sup>+</sup> and **(h)** CD8<sup>+</sup>CD69<sup>+</sup> T cells in mice. Circulating plasma levels of **(i)** MCP1, **(j)** TNF $\alpha$  and **(k)** IL6. Representative scatter plots of the gating strategy used for the flow cytometry analysis for the different leucocyte populations, monocyte subsets and subtypes of T lymphocytes are shown. Statistical analysis was performed using Student's *t* test. White bars, vehicle-treated mice, *n* = 11; black bars, lixisenatide-treated mice, *n* = 14. \**p* < 0.05 and \*\**p* < 0.01 vs vehicle



contrast, iNOS was significantly decreased following lixisenatide treatment (Fig. 8f). Consistent with these results, the ratio of arginase I/iNOS-stained area in atheromas was higher in lixisenatide-treated vs vehicle-treated *Apoe<sup>-/-</sup>Irs2<sup>+/-</sup>* mice (Fig. 8g). Analysis of double Mac-3/arginase I and Mac-3/iNOS immunofluorescence showed the presence of macrophages expressing arginase I and iNOS proteins in both vehicle- and lixisenatide-treated mice (Fig. 8d). Therefore, lixisenatide promotes an M2 macrophage phenotype in vivo in *Apoe<sup>-/-</sup>Irs2<sup>+/-</sup>* mouse atheromas.

## Discussion

The average reduction in life expectancy of a person with type 2 diabetes is approximately 10 years, due mainly to CVD. Recent clinical trials indicate that therapies based on the GLP-1/GLP-1-receptor axis may represent useful treatments to reduce the risk of CVD [11, 13, 19]. In our study, treating *Apoe<sup>-/-</sup>Irs2<sup>+/-</sup>* mice (which develop characteristics of IR, the

metabolic syndrome and accelerated atherosclerosis) with lixisenatide or liraglutide efficiently decreased atherosclerosis, indicating a drug class effect. Atheromas from lixisenatide-treated mice also displayed characteristics of stable plaques, diminished inflammatory cell infiltration, smaller necrotic cores and thicker fibrous caps. As expected, lixisenatide and liraglutide alleviated IR and improved blood pressure but did not change body weight loss or plasma lipid levels. Lixisenatide treatment also reduced markers of systemic inflammation, including proinflammatory Ly6C<sup>hi</sup>-monocytes, activated T cells and IL-6 cytokine plasma levels. Moreover, lixisenatide modulated macrophage polarisation towards an M2 phenotype, as *Apoe<sup>-/-</sup>Irs2<sup>+/-</sup>* mouse macrophages differentiated with the drug exhibited enhanced levels of activated STAT3 and diminished activated STAT1 in response to LPS. Consistently, in vitro treatment of macrophages with lixisenatide resulted in decreased secretion of M1 macrophage-derived IL-6 cytokine, reduced iNOS levels (an enzyme that characterises M1 macrophages) and augmented expression of arginase I (an M2 marker). In agreement with a



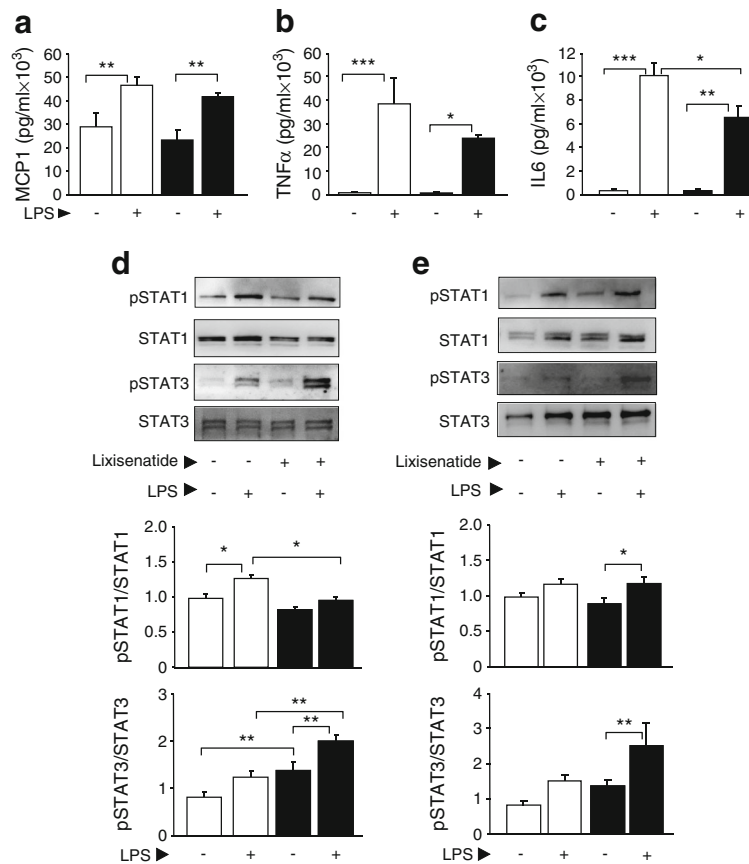


**Fig. 7** Inflammatory properties of *Apoe*<sup>-/-</sup>*Irs2*<sup>+/-</sup> mouse macrophages treated with lixisenatide. (**a–c**) Secretion of proinflammatory cytokines MCP1 (**a**), TNF $\alpha$  (**b**) and IL6 (**c**) in *Apoe*<sup>-/-</sup>*Irs2*<sup>+/-</sup> mouse macrophages treated with 40 nmol/l lixisenatide or vehicle in basal conditions and when stimulated with LPS (100 ng/ml) for 6 h ( $n = 8$ ). (**d, e**) Quantification of protein expression of the activated (phosphorylated) forms of the STAT1 and STAT3 transcription factors in vehicle- and

40 nmol/l lixisenatide-treated macrophages stimulated with saline or with LPS (100 ng/ml) for 6 h (**d**;  $n = 5–11$ ) or 24 h (**e**;  $n = 4–10$ ). Phosphorylated forms were normalized to the total STAT1 and STAT3 protein levels. Representative blots are shown. Statistical analysis was performed using two-way ANOVA test followed by Tukey's post hoc test. White bars, vehicle-treated macrophages; black bars, lixisenatide-treated macrophages. \* $p < 0.05$ , \*\* $p < 0.01$ , \*\*\* $p < 0.001$  as indicated

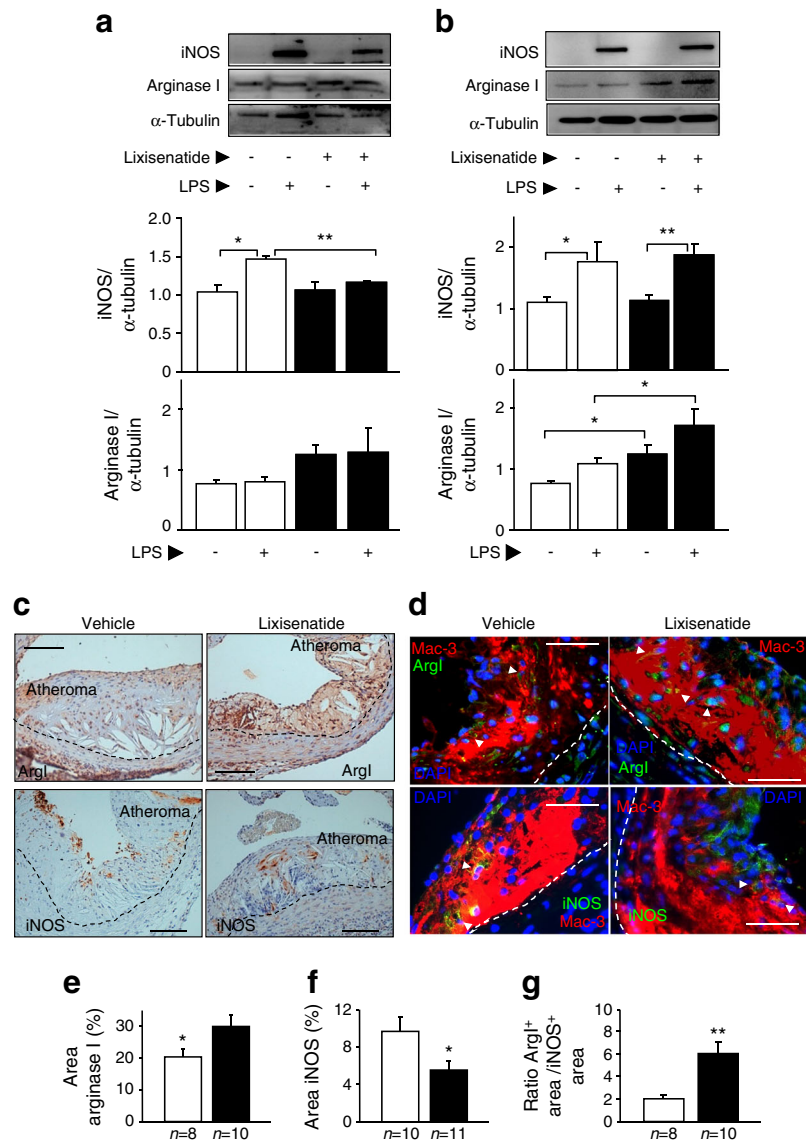
role for lixisenatide in macrophage reprogramming, higher arginase I and lower iNOS levels were also detected in vivo in atheromas from lixisenatide-treated *Apoe*<sup>-/-</sup>*Irs2*<sup>+/-</sup> mice. Our results demonstrate that the GLP-1 analogue lixisenatide plays a relevant role in the reprogramming of macrophage fate towards an anti-inflammatory M2 phenotype; this might also represent a key mechanism for decreased atherosclerosis and acute cardiovascular events associated with IR.

Previous studies have shown that liraglutide treatment decreases atherosclerosis in *Apoe*<sup>-/-</sup> mice [12, 28, 29] and in LDL-receptor-deficient mice [30] but also improves endothelial dysfunction [31–33]. However, this is the first study to evaluate the impact of GLP1 analogues on atherosclerosis in the context of IR and to provide a mechanistic insight into the cardiovascular actions of the incretin-based therapies in vivo. Thus, treatment with lixisenatide or liraglutide markedly decreased atherosclerosis in IR *Apoe*<sup>-/-</sup>*Irs2*<sup>+/-</sup> mice. In addition, lixisenatide treatment improved some markers of plaque stability; lower macrophage and T cell contents were observed, an important finding because these are the predominant cell

types in plaque rupture and erosion sites [34]. These results are consistent with the LEADER clinical trial, which revealed that individuals with type 2 diabetes treated with the GLP-1 analogue liraglutide had lower death rates from cardiovascular causes [13].

As expected, lixisenatide and liraglutide alleviated IR and improved blood pressure in *Apoe*<sup>-/-</sup>*Irs2*<sup>+/-</sup> mice. However, no changes were observed in body weight or plasma lipid levels, indicating that the reduction in CVD produced by these drugs does not result from an improvement in lipid metabolism or reduced fat content. The lack of an effect on body weight could be attributed to the absence of obesity in the *Apoe*<sup>-/-</sup>*Irs2*<sup>+/-</sup> mouse model. This is not unprecedented as previous studies have reported no changes in body weight using these drugs in different animal models of obesity and diabetes [15, 30]. Our results support and extend previous data indicating the complex biology of the GLP-1/GLP-1-receptor pathway in the cardiovascular system and highlight its potential beneficial effects in addition to its main function through the enteroinsular axis [9].

**Fig. 8** Effect of lixisenatide on *Apoe<sup>-/-</sup>Irs2<sup>+/-</sup>* mouse macrophage polarisation. (**a, b**) Quantification of protein expression of iNOS and arginase I content in vehicle- and 40 nmol/l lixisenatide-treated macrophages stimulated with saline or with LPS (100 ng/ml) for 6 h (**a**;  $n = 3-12$ ) or 24 h (**b**;  $n = 3-11$ ). Protein levels were normalised to  $\alpha$ -tubulin protein levels. Representative blots are shown. (**c**) Representative images of the arginase I (ArgI) and iNOS stains used for quantifications in (**e-g**) and (**d**) double Mac-3/ArgI and Mac-3/iNOS immunofluorescence showing macrophages expressing ArgI and iNOS proteins. Arrowheads indicate double Mac-3<sup>+</sup>ArgI<sup>+</sup> and Mac-3<sup>+</sup>iNOS<sup>+</sup> areas. The dashed lines delineate the limits of the media. Quantification of arginase I content (**e**) and iNOS content (**f**) (expressed as % of atheroma area stained positive); and arginase I/iNOS ratio (**g**) in atheromas of lixisenatide- and vehicle-treated *Apoe<sup>-/-</sup>Irs2<sup>+/-</sup>* mice. Statistical analysis was performed using one-way ANOVA followed by Tukey's post hoc test (**a, b**) and Student's *t* test (**e-g**). White bars, vehicle-treated macrophages or mice; black bars, lixisenatide-treated macrophages or mice. Scale bars, 100  $\mu$ m (**c**) or 50  $\mu$ m (**d**). \* $p < 0.05$  and \*\* $p < 0.01$  as indicated or vs vehicle



Given that GLP-1 hormone promotes pancreatic beta cell [9] and cardiomyocyte [35] survival, we hypothesised that the GLP-1 analogue lixisenatide could affect vessel-wall cell survival. However, treatment with this drug did not affect the macrophage proliferation rate. Previous studies have shown that increased endoplasmic reticulum stress-induced macrophage apoptosis is a relevant molecular mechanism of atheroma plaque vulnerability in states of IR [1, 6]. However, in vivo analysis of apoptosis revealed that lixisenatide does not affect this process in atheromas from *Apoe<sup>-/-</sup>Irs2<sup>+/-</sup>* mice. Nevertheless, we cannot discard the possibility that lixisenatide might affect macrophage survival in more advanced plaques.

Classically activated M1 macrophages exhibit atherogenic activity by secreting proinflammatory cytokines such as TNF $\alpha$  and IL-6 and modulating plaque rupture susceptibility

through their preferential location in plaque shoulders [36]. In contrast, M2 macrophages have main functions in tissue repair and resolution of inflammation and also downregulate M1-associated cytokines [27, 37]. Switching of the M1 macrophage phenotype involves alteration of the activation status of the MAPK and STAT signalling pathways, among several other changes [27]. Macrophages differentiated in the presence of lixisenatide displayed higher levels of activated STAT3 protein and lower LPS-stimulated STAT1 activation; these transcription factors are essential for modulating M2 and M1 phenotype shift, respectively. In contrast, MAPK activation analysis showed the drug to have no effect on these pathways. Thus, lixisenatide might promote plaque stability through a mechanism that modulates the STAT signalling pathway resulting in the reprogramming of macrophages. In fact, lixisenatide-differentiated macrophages secreted less IL-

6 upon LPS stimulation and displayed increased levels of the M2 macrophage marker arginase I and reduced expression of the M1 macrophage marker iNOS. These findings correlate well with data from previous *in vitro* studies using human macrophages describing the anti-inflammatory effects of exenatide [38], and with other work in a mouse model of diet-induced obesity indicating that a related incretin-based therapy, the DPP-4 inhibitor linagliptin, reduces IR through an anti-inflammatory action [39]. Interestingly, in this later study, linagliptin did not change circulating Ly6C subpopulations, indicating that DPP-4 inhibitors do not modulate recruitment of monocytes into the blood. Thus, the anti-inflammatory actions of linagliptin were attributed to an M2 shift of macrophages within insulin-sensitive tissues by a mechanism that included a reduction in the production of reactive oxygen species and subsequent attenuation of systemic IR. In contrast, we found that lixisenatide decreased circulating Ly6C<sup>hi</sup> monocytes, lowered activated T cells and, during bone-marrow macrophage differentiation, induced an M2 phenotype with enhanced arginase I expression and STAT3 activation. Thus, these studies suggest that the mechanism of action of GLP-1 analogues could include the *in vivo* reprogramming of the immune stem cell fate, having a major effect on systemic inflammation.

In line with the above results, analysis of circulating cytokines in lixisenatide-treated mice revealed a decrease in IL-6, a target cytokine for many anti-inflammatory therapies, whose signalling pathway is hypothesised to be critical in inflammation associated with atherosclerosis [34]. Moreover, lixisenatide treatment decreased iNOS but enhanced the presence of arginase I in atheromas; these changes correlated with an increase in plaque stability. This finding is consistent with recent work demonstrating that infusion of arginase I in mice decreases the secretion of the proinflammatory IL-6 cytokine, reduces iNOS levels and produces more stable plaques, characterised by the presence of thicker fibrous caps [40]. Altogether, these results suggest that the GLP-1/GLP-1 receptor axis plays a critical function in decreasing atherosclerosis and might promote plaque stability through modulation of the macrophage phenotype in an arginase I-dependent manner.

In summary, our data shows that lixisenatide modulates the activation of STAT-dependent pathways and provides mechanistic insights to suggest a function for the GLP-1/GLP-1 receptor axis in the reprogramming of macrophages towards an M2 phenotype. In addition, we showed that this lixisenatide-mediated effect is a main *in vivo* molecular mechanism of the atheroma plaque size reduction in insulin-resistant mice treated with this drug. Thus, this present study provides experimental evidence for the use of GLP-1 analogues as potential therapeutic agents to reduce cardiovascular residual risk and acute events in individuals exhibiting characteristics of type 2 diabetes and suggests a potential use of these therapies in personalised therapies.

**Acknowledgements** We thank G. Herrera (Central Unit for Research in Medicine, INCLIVA, Spain) for assistance with the flow cytometry analysis and A. Diaz (Central Unit for Research in Medicine, University of Valencia, Spain) for help with animal care.

**Data availability** Data are available upon reasonable request to the corresponding authors.

**Funding** This study was supported by grants from the Carlos III Health Institute (PI13/00834, PI16/00091 awarded to HG-N) and the European Regional Development Fund (FEDER) and by a research grant from Sanofi-Aventis to HG-N. HG-N is an investigator in the Miguel Servet program (CP10/00555 and CP16/00013). AV and AH-C received salary support from the European Foundation for the Study of Diabetes and from Proyecto Paula. This work was also supported by CIBERDEM (CB07/08/0043), a Carlos III Health Institute initiative.

**Duality of interest** HG-N received research support from Sanofi-Aventis through INCLIVA. All other authors declare that there is no duality of interest associated with their contribution to this manuscript.

**Contribution statement** AV acquired and analysed the *in vivo* data, participated in the interpretation of results and helped to write the manuscript. JN participated in the study design, helped to interpret the data and helped to write the manuscript. MG-C performed *in vitro* and immunofluorescent experiments and revised the manuscript. AH-C and IA-B performed flow cytometry experiments and inflammatory characterisation, interpreted the data and helped to write the manuscript. SM-H, JFA and JTR participated in the design of the study and critically revised the manuscript. HG-N conceived and designed the study, supervised the data acquisition, interpreted the results and wrote the manuscript. All the authors approved the final version of the manuscript. HG-N is the guarantor of this work.

## References

1. Bornfeldt KE (2015) Uncomplicating the macrovascular complications of diabetes: the 2014 Edwin Bierman award lecture. *Diabetes* 64:2689–2697
2. Libby P, Pasterkamp G (2016) Requiem for the vulnerable plaque. *Eur Heart J* 36:2984–2987
3. Baumgartl J, Baudler S, Scherner M et al (2006) Myeloid lineage cell-restricted insulin resistance protects apolipoprotein E-deficient mice against atherosclerosis. *Cell Metab* 3:247–256
4. Gonzalez-Navarro H, Vila-Caballer M, Pastor MF et al (2007) Plasma insulin levels predict the development of atherosclerosis when IRS2 deficiency is combined with severe hypercholesterolemia in apolipoprotein E-null mice. *Front Biosci* 12:2291–2298
5. Han S, Liang CP, DeVries-Seimon T et al (2006) Macrophage insulin receptor deficiency increases ER stress-induced apoptosis and necrotic core formation in advanced atherosclerotic lesions. *Cell Metab* 3:257–266
6. Martinez-Hervas S, Vinue A, Nunez L et al (2014) Insulin resistance aggravates atherosclerosis by reducing vascular smooth muscle cell survival and increasing CX3CL1/CX3CR1 axis. *Cardiovasc Res* 103:324–336
7. van Dijk RA, Duiniveld AJ, Schaapherder AF et al (2015) A change in inflammatory footprint precedes plaque instability: a systematic evaluation of cellular aspects of the adaptive immune response in human atherosclerosis. *J Am Heart Assoc* 4:e001403

8. Maurovich-Horvat P, Ferencik M, Voros S, Merkely B, Hoffmann U (2014) Comprehensive plaque assessment by coronary CT angiography. *Nat Rev Cardiol* 11:390–402
9. Drucker DJ (2006) The biology of incretin hormones. *Cell Metab* 3:153–165
10. Campbell JE, Drucker DJ (2013) Pharmacology, physiology, and mechanisms of incretin hormone action. *Cell Metab* 17:819–837
11. Wohlfart P, Linz W, Hubschle T et al (2013) Cardioprotective effects of lixisenatide in rat myocardial ischemia-reperfusion injury studies. *J Transl Med* 11:84
12. Tashiro Y, Sato K, Watanabe T et al (2014) A glucagon-like peptide-1 analog liraglutide suppresses macrophage foam cell formation and atherosclerosis. *Peptides* 54:19–26
13. Marso SP, Daniels GH, Brown-Frandsen K et al (2016) Liraglutide and cardiovascular outcomes in type 2 diabetes. *N Engl J Med* 375:311–322
14. Pfeiffer MA, Claggett B, Diaz R et al (2015) Lixisenatide in patients with type 2 diabetes and acute coronary syndrome. *N Engl J Med* 373:2247–2257
15. Thorkildsen C, Neve S, Larsen BD, Meier E, Petersen JS (2003) Glucagon-like peptide 1 receptor agonist ZP10A increases insulin mRNA expression and prevents diabetic progression in db/db mice. *J Pharmacol Exp Ther* 307:490–496
16. Werner U, Haschke G, Herling AW, Kramer W (2010) Pharmacological profile of lixisenatide: a new GLP-1 receptor agonist for the treatment of type 2 diabetes. *Regul Pept* 164:58–64
17. Larsen PJ, Fledelius C, Knudsen LB, Tang-Christensen M (2001) Systemic administration of the long-acting GLP-1 derivative NN2211 induces lasting and reversible weight loss in both normal and obese rats. *Diabetes* 50:2530–2539
18. Noyan-Ashraf MH, Momen MA, Ban K et al (2009) GLP-1R agonist liraglutide activates cytoprotective pathways and improves outcomes after experimental myocardial infarction in mice. *Diabetes* 58:975–983
19. Noyan-Ashraf MH, Shikatani EA, Schuiki I et al (2013) A glucagon-like peptide-1 analog reverses the molecular pathology and cardiac dysfunction of a mouse model of obesity. *Circulation* 127:74–85
20. Martorell S, Hueso L, Gonzalez-Navarro H, Collado A, Sanz MJ, Piqueras L (2016) Vitamin D receptor activation reduces angiotensin-ii-induced dissecting abdominal aortic aneurysm in apolipoprotein E-knockout mice. *Arterioscler Thromb Vasc Biol* 36:1587–1597
21. Gonzalez-Navarro H, Nong Z, Amar MJ et al (2004) The ligand-binding function of hepatic lipase modulates the development of atherosclerosis in transgenic mice. *J Biol Chem* 279:45312–45321
22. Gonzalez-Navarro H, Vinue A, Sanz MJ et al (2013) Increased dosage of Ink4/Arf protects against glucose intolerance and insulin resistance associated with aging. *Aging Cell* 12:102–111
23. Vinue A, Andres-Blasco I, Herrero-Cervera A et al (2015) Ink4/Arf locus restores glucose tolerance and insulin sensitivity by reducing hepatic steatosis and inflammation in mice with impaired IRS2-dependent signalling. *Biochim Biophys Acta* 1852:1729–1742
24. Gonzalez-Navarro H, Abu Nabah YN, Vinue A et al (2010) p19(ARF) deficiency reduces macrophage and vascular smooth muscle cell apoptosis and aggravates atherosclerosis. *J Am Coll Cardiol* 55:2258–2268
25. Andres-Blasco I, Vinue A, Herrero-Cervera A et al (2016) Hepatic lipase inactivation decreases atherosclerosis in insulin resistance by reducing LIGHT/lymphotoxin  $\beta$ -receptor pathway. *Thromb Haemost* 116:379–393
26. Jin Y, Liu Y, Nelin LD (2015) Extracellular signal-regulated kinase mediates expression of arginase II but not inducible nitric-oxide synthase in lipopolysaccharide-stimulated macrophages. *J Biol Chem* 290:2099–2111
27. Sica A, Mantovani A (2012) Macrophage plasticity and polarization: in vivo veritas. *J Clin Invest* 122:787–795
28. Arakawa M, Mita T, Azuma K et al (2010) Inhibition of monocyte adhesion to endothelial cells and attenuation of atherosclerotic lesion by a glucagon-like peptide-1 receptor agonist, exendin-4. *Diabetes* 59:1030–1037
29. Gaspari T, Welungoda I, Widdop RE, Simpson RW, Dear AE (2013) The GLP-1 receptor agonist liraglutide inhibits progression of vascular disease via effects on atherogenesis, plaque stability and endothelial function in an ApoE<sup>-/-</sup> mouse model. *Diab Vasc Dis Res* 10:353–360
30. Bisgaard LS, Bosteen MH, Fink LN et al (2016) Liraglutide reduces both atherosclerosis and kidney inflammation in moderately uremic LDLr<sup>-/-</sup> mice. *PLoS One* 11:e0168396
31. Shiraki A, Oyama J, Komoda H et al (2012) The glucagon-like peptide 1 analog liraglutide reduces TNF- $\alpha$ -induced oxidative stress and inflammation in endothelial cells. *Atherosclerosis* 221:375–382
32. Dai Y, Mehta JL, Chen M (2013) Glucagon-like peptide-1 receptor agonist liraglutide inhibits endothelin-1 in endothelial cell by repressing nuclear factor-kappa B activation. *Cardiovasc Drugs Ther* 27:371–380
33. Krasner NM, Ido Y, Ruderman NB, Cacicedo JM (2014) Glucagon-like peptide-1 (GLP-1) analog liraglutide inhibits endothelial cell inflammation through a calcium and AMPK dependent mechanism. *PLoS One* 9:e97554
34. Ridker PM, Luscher TF (2014) Anti-inflammatory therapies for cardiovascular disease. *Eur Heart J* 35:1782–1791
35. Ussher JR, Drucker DJ (2014) Cardiovascular actions of incretin-based therapies. *Circ Res* 114:1788–1803
36. Stoger JL, Gijbels MJ, van der Velden S et al (2012) Distribution of macrophage polarization markers in human atherosclerosis. *Atherosclerosis* 225:461–468
37. Kim HS, Tavakoli S, Piefer LA, Nguyen HN, Asmis R (2016) Monocytic MKP-1 is a sensor of the metabolic environment and regulates function and phenotypic fate of monocyte-derived macrophages in atherosclerosis. *Sci Rep* 6:34223
38. Shiraishi D, Fujiwara Y, Komohara Y, Mizuta H, Takeya M (2012) Glucagon-like peptide-1 (GLP-1) induces M2 polarization of human macrophages via STAT3 activation. *Biochem Biophys Res Commun* 425:304–308
39. Zhuge F, Ni Y, Nagashimada M et al (2016) DPP-4 inhibition by linagliptin attenuates obesity-related inflammation and insulin resistance by regulating M1/M2 macrophage polarization. *Diabetes* 65:2966–2979
40. Wang XP, Zhang W, Liu XQ et al (2014) Arginase I enhances atherosclerotic plaque stabilization by inhibiting inflammation and promoting smooth muscle cell proliferation. *Eur Heart J* 35:911–919